Pre-Print Manuscript of Article:

Bridgelall, R., Rahman, T., Daleiden, J. F., Tolliver, D., "Error sensitivity of the connected vehicle approach to pavement performance evaluations," *International Journal of Pavement Engineering*, pp. 1-6, March 28, 2016.

Error sensitivity of the connected vehicle approach to pavement performance evaluations

Raj Bridgelall[1], Md Tahmidur Rahman[2], Jerome F. Daleiden[3], Denver Tolliver[4]

Upper Great Plains Transportation Institute, North Dakota State University, Fargo, ND, USA
Fugro Roadware Inc., Austin, TX, USA

[1]Raj Bridgelall (Corresponding Author):

P.O. Box 863676, Plano, TX, 75086; Phone 408-607-3214; E-mail: raj@bridgelall.com

[2]Fugro Roadware, Inc., 8613 Cross Park Drive, Austin, TX 78754; Phone: 512-977-1879; Email: trahman@fugro.com

[3]Jerome F. Daleiden: Fugro Roadware, Inc., 8613 Cross Park Drive, Austin, TX 78754; Phone: 512-977-1800; Email: jdaleiden@fugro.com

[4]Denver Tolliver: P.O. Box 6050, Fargo, ND 58108; Phone 701-231-7190; E-mail: denver.tolliver@ndsu.edu

The University Transportation Centre, a program of the United States Department of Transportation, sponsored this research through its Mountain Plains Consortium (MPC) under grant DTRT12-G-UTC08.

Abstract

The international roughness index is the prevalent indicator used to assess and forecast road maintenance needs. The fixed parameters of its simulation model provide the advantage of requiring relatively few traversals to produce a consistent index. However, the static parameters also cause the model to under-represent roughness that riders experience from profile wavelengths outside of the model's response range. A connected vehicle method that uses a similar but different index to characterize roughness can do so by accounting for all vibration wavelengths that the actual vehicles experience. This study characterizes and compares the precision of each method. The field studies indicate that within 7 traversals, the connected vehicle approach could achieve the same level of precision as the procedure used to produce the international roughness index. For a given vehicle and segment lengths longer than 50 meters, the margin-of-error diminished below 1.5% after 50 traversals, and continued to improve further as the traversal volume grew. Practitioners developing new tools to evaluate pavement performance will benefit from this study by understanding the precision trade-off to recommend best practices in utilizing the connected vehicle method.

Keywords: connected vehicle; GPS; inertial profiler; measurement precision; pavement management; probe vehicles; ride quality; smartphone

1 Introduction

Transportation agencies rely on the regular reporting of pavement performance to prioritize maintenance needs. Existing methods of smoothness (or roughness) characterizations that use the international roughness index (IRI) are difficult or impractical to apply on unpaved roads and in most urban settings (Karamihas 2015). In particular, interrupted flow conditions generally diminish the accuracy of the present data collection methods. These deficiencies coupled with the relatively high cost to acquire, maintain, and operate inertial profilers has motivated the search for alternative methods. Subsequently, transportation agencies are evaluating connected vehicle approaches because of their potential to provide affordable, continuous, and network-wide coverage. Connected vehicle methods rely on the inertial and geospatial position data from common on-board accelerometers and GPS receivers. The authors previously developed and demonstrated the road impact factor (RIF) transform to process voluminous data from connected vehicle sources (Bridgelall 2014a). The transform is a mathematical model that integrates the inertial, speed, and geospatial position data streams across a given segment length to produce a roughness index called the RIF-index. Other work described the theories and experiments showing that within any selected speed band, RIF-indices are directly proportional to the IRI (Bridgelall 2014b).

Practitioners have long recognized that the IRI mischaracterizes roughness that riders experience (Ahlin and Granlund 2002). Specifically, the fixed quarter-car (Golden Car) parameters and the precise reference speed of the IRI procedure result in a spatial wavelength bias (Papagiannakis 1997). Traversing spatial wavelengths at different speeds produce temporal wavelengths at frequencies that coincide with the resonant modes of vehicle suspension system to amplify ride roughness (Lak, Degrande and Lombaert 2011).

The RIF-transform precludes wavelength bias by reporting the roughness that riders actually experienced at the speed that they travelled, and in their real vehicles (Bridgelall 2015). Unlike the IRI that uses a precise speed of 80 km h^{-1}, the RIF-transform uses the actual speed travelled. Therefore, the notation for RIF-indices includes a subscript to indicate the average traversal speed in a speed band. Previous studies described the trade-off in selecting the width of the speed band, and the number of traversals needed to achieve some desired level of precision (Bridgelall 2015).

The average RIF-index from a specified speed band is analogous to the average IRI reported from multiple traversals of a facility. As anticipated, the fixed quarter-car model and the precise reference speed of 80 km h^{-1} results in a relatively high consistency of IRI reporting. Conversely, the connected vehicle method reflects variations in the actual speed, suspension system behaviour, and sensor characteristics.

The main objectives of this study are to:

(1) characterize the practically achievable precision of the connected vehicle method,

(2) identify the dominant parameters that contribute to precision dilution,

(3) evaluate the relative impacts from each parameter, and

(4) quantify the number of traversals needed to report RIF-indices with the same level of precision as the IRI procedure.

Previous work examined the impact from variations in accelerometer sample rate, vehicle speed, and suspension system performance for a typical mix of vehicles in the traffic stream. Those studies found that the dilution of precision becomes insignificant when the sample rate of the accelerometer exceeds 64 Hertz (Bridgelall 2015), and when the traversal volume exceeds 50 (Bridgelall 2014b). The method of this study isolates the impact from variation in the analysed traversal path by fixing the accelerometer sample rate to a value much higher than 64 Hertz, using the same vehicle for multiple traversals, and traveling the same test segment with more careful speed regulation. Practitioners developing new tools to evaluate pavement performance will benefit from this study by understanding the trade-off to produce guidelines for best practices when deploying the connected vehicle methods.

The organization of this paper is as follows: the next section will review the RIF-transform and theoretically characterize the significance of factors that dilute the precision of measurements. The third section will describe the field experiments conducted to quantify the relative impact from variations in the analysed traversal path. The fourth section will discuss the trade-off in precision and traversal volume as a function of the minimum segment length analysed. The final section will summarize and conclude the study.

2 The connected vehicle approach to measuring pavement roughness

Given the highly specialized area of pavement performance evaluations, few other researchers have developed methods to transform sensor data from connected vehicles to characterize roughness. Previous work that attempted to relate the accelerometer signal to the IRI witnessed a speed dependency but did not establish a mathematical characterization to explain the behaviour observed (Dawkins *et al.* 2011, Du *et al.* 2014). Related research investigated participatory sensing approaches that would identify clusters of roughness reports from riders to suggest the locations of possible anomalies such as potholes (Byrne *et al.* 2013). Methods that directly analyse the accelerometer signal stream from individual vehicles used short-time spectral transforms to identify the signatures of anomalies (Ayenu-

Prah and Attoh-Okine 2009). Some methods attempt to recover the road profile by double integration of the accelerometer signal (Islam *et al*. 2014, Nomura and Shiraishi 2015). Approaches that are more recent investigated signal classification via machine learning techniques to identify possible anomalies (Rajamohan, Gannu and Rajan 2015).

The next sections review the connected vehicle method of characterizing pavement roughness in terms of the RIF-index. Previous work (Bridgelall et al. 2014) established that the fusion of sensor data from many connected vehicles is a primary factor in its superiority over other approaches that can afford very few traversals. The derivation of a model to characterize the individual error contributors will establish a framework to guide the design of field experiments and the data processing to quantify the proportional error contributions.

2.1 Inertial signal transformation

For individual vehicle traversals, the RIF-transform produces a measure of localized roughness such that

$$R_{\bar{v}}^{L} = \sqrt{\frac{1}{L}\sum_{n=0}^{N-1}\left|g_{z[n]}v_n\right|^2 \delta t} \tag{1}$$

where the RIF-index $R_{\bar{v}}^{L}$ is the average g-force magnitude experienced per unit of distance L when travelling at an average speed of $\bar{v}$ (Bridgelall 2014a). An on-board accelerometer produces the vertical acceleration $g_{z[n]}$ for signal sample n of N total samples. A speed sensor produces the instantaneous traversal speed v_n. Previous research established that the average sample period δt should be at least 64 Hertz (Bridgelall 2014b). Increasing the sample rate beyond 64 Hertz does increase the level of measurement consistency for a given traversal volume, but with diminishing returns beyond 100 Hertz.

For situations when speed variation is not a dominant factor in precision dilution, the expression for the RIF-transform is simplified by replacing the instantaneous speed with the average speed such that

$$R_{\bar{v}}^{L} = \bar{v}\sqrt{\frac{1}{L}\sum_{n=0}^{N-1}\left|g_{z[n]}\right|^{2}\delta t} \tag{2}$$

Let the linear energy density be defined as

$$E_{gz}^{L} = \frac{1}{L}\sum_{n=0}^{N-1}\left|g_{z[n]}\right|^{2}\delta t \tag{3}$$

that is, the signal energy per meter travelled. Hence, the units are in joules per meter when the output of the accelerometer signal is a voltage. Subsequently, for an average speed, the simplified RIF-transform is

$$R_{\bar{v}}^{L} = \bar{v}\sqrt{E_{gz}^{L}}\,. \tag{4}$$

In the trivial case where the traversal speed is zero, the RIF-index must be zero.

It is important to distinguish this expression from the root-mean-square (RMS) of the signal samples. That is, the RMS is the square root of the signal energy per unit of *time* rather than distance. Substituting $L = \bar{v}T$ into Equation (2) reveals the relationship with the RMS of the accelerometer signal. That is,

$$R_{\bar{v}}^{L} = \sqrt{\bar{v}}\sqrt{\frac{1}{T}\sum_{n=0}^{N-1}\left|g_{z[n]}\right|^{2}\delta t} = \sqrt{\bar{v}}\,g_{z\_\mathrm{rms}} \tag{5}$$

where T is the total traversal time of segment L, traveling at the average speed. This subtle distinction is important and critical to expressing the non-linear behaviour of the accelerometer output at different speeds.

2.2 Variance in measurements

For a constant speed and a fixed quarter-car, the IRI will vary with differences in the elevation profile measurements among traversals. However, variations in the RIF-indices will include the effects of speed fluctuations. Other sources of errors include variations in the traversal path, inertial sample interval, and vehicle suspension responses. From the classical theory of error propagation (Papoulis 1991), the standard deviation of the RIF-index, σ_R^L is:

$$\sigma_R^L = \sqrt{\left(\frac{\partial R_{\bar{v}}^L}{\partial \bar{v}}\right)^2 \sigma_{\bar{v}}^2 + \left(\frac{\partial R_{\bar{v}}^L}{\partial E_{\mathrm{gz}}^L}\right)^2 \mathrm{Var}\left[E_{\mathrm{gz}}^L\right] + \left(\frac{\partial R_{\bar{v}}^L}{\partial \bar{v}}\right)\left(\frac{\partial R_{\bar{v}}^L}{\partial E_{\mathrm{gz}}^L}\right)\sigma_{\bar{v}E}^2} \tag{6}$$

where $\sigma_{\bar{v}}^2$ is the variance of the batch mean speed among traversals. The covariance of the batch mean speed and the vertical acceleration signal energy is denoted $\sigma_{\bar{v}E}^2$. Evaluating the partial derivatives indicated in Equation (6) yields:

$$\sigma_R^L = \sqrt{\bar{E}_{\mathrm{gz}}^L \sigma_{\bar{v}}^2 + \left(\bar{\bar{v}}/2\right)^2 \frac{\mathrm{Var}\left[E_{\mathrm{gz}}^L\right]}{\bar{E}_{\mathrm{gz}}^L} + \left(\bar{\bar{v}}/2\right)\sigma_{\bar{v}E}^2} \tag{7}$$

where $\bar{E}_{\mathrm{gz}}^L$ and $\bar{\bar{v}}$ are the averages of the linear energy density of the vertical acceleration signal and the batch mean speed among traversals, respectively.

2.3 Proportional contribution to the spread in RIF-indices

From equation (7), the proportional error contribution from variations in speed η_v^L is

$$\eta_{\mathrm{v}}^{L} = \overline{E}_{gz}^{L}\left(\frac{\sigma_{\overline{v}}}{\sigma_{R}^{L}}\right)^{2} \tag{8}$$

Therefore, the proportional contribution from the remaining errors η_{E}^{L} will be

$$\eta_{\mathrm{E}}^{L} = 1 - \overline{E}_{gz}^{L}\left(\frac{\sigma_{\overline{v}}}{\sigma_{R}^{L}}\right)^{2}. \tag{9}$$

We define the residual error η_{E}^{L} as all contributions to the spread in RIF-indices that result from variations other than speed. Hence, given a precise speed, the residual errors will reflect variations in the traversal path, fluctuations in the sample interval, and variations in the vehicle suspension response. Using the same vehicle and sensor for all traversals will minimize variations in the suspension behaviour and the sample interval, respectively. Therefore, variations in the length and position of the traversal path would expectedly dominate the aggregate error observed.

2.4 Geo-fence triggering

Connected vehicles use geo-fences to establish the lateral positions from where agencies wish to characterize and report roughness (Bridgelall 2015). As shown in figure 1, a lateral geo-fence at position L_0 identifies the start of the data section to be analysed.

For a fixed GPS update rate, the actual starting position in the geospatially tagged data stream will vary about the precise geo-fence position as illustrated in figure 1. The final data point will be located at an interpolated segment length L_n such that

$$L_n = L_0 + \sum_{k=1}^{n} v_k t_k \tag{10}$$

where v_k and t_k are the instantaneous speed and time updates for the k^{th} inertial sample. Figure 1 illustrates this data acquisition approach for two different path lengths L_a and L_b such that $L_\text{b} >> L_\text{a}$. Each line represents the geospatial position and length of the segment to be analysed from traversal data stream n. The length of the error interval L_σ depends on the GPS update rate, the statistics of the GPS position estimate, and the traversal speed. The corresponding variations in traversal path positions and lengths translate to variations in the RIF-indices reported.

[Figure 1 near here].

Figure 1 illustrates a hypothetical elevation profile that would produce obvious variations in RIF-indices for the shorter path L_a, but not for the longer path L_b. That is, the shorter paths shown include the anomalies to varying degrees. Therefore, the corresponding set of RIF-indices $\left\{R_{\bar{v}}^{L_\text{a}}[1] \cdots R_{\bar{v}}^{L_\text{a}}[n]\right\}$ will reflect the proportion of the rough spot that the analysed path covers. Conversely, the longer path always includes all of the anomalies. Therefore, for fixed path lengths, the RIF-indices for the longer path in this scenario will exhibit no variation.

3 Case studies

The Minnesota Road Research Facility (MnROAD) is an outdoor laboratory that the Minnesota Department of Transportation operates in the U.S. to test the performance of different pavement types (MnROAD 2015). On June 10, 2015, the authors used a certified and approved inertial profiler to collect simultaneously elevation profile and vertical acceleration data from a 70-meter section of Cell 40 to produce the IRI and RIF-indices, respectively. The pavement analysis via vehicle electronic telemetry (PAVVET) application (app) for a smartphone (Bridgelall 2014c) collected the inertial and speed data at a mean sample rate of 93 Hertz, which was the maximum that the device could practically achieve. The device internally established a mean GPS update interval of approximately 1 second. The app collected data with the smartphone secured into a holster attached to the dashboard. The mean traversal speed of the inertial profiler was 80 km h^{-1}.

Table 1 summarizes the IRI and RIF-indices derived from the measurements. The inertial profiler was available to collect data for only $N = 9$ traversals. Operating errors on two of the traversals resulted in smartphone data losses, so those entries are not available in the table.

[Table 1 near here].

To examine the data consistency, the analysis incorporated a larger PAVVET data set available from an experiment conducted on Cell 40 three months prior (Bridgelall *et al.* 2016). The data set contained 53 traversal samples from a 2011 Chevrolet Traverse. The mean speed was 68 km h^{-1} (~42 mph) and the PAVVET app settings were identical. Table 2 characterizes the roughness from the 70-meter traversals (last row), and the roughness across shorter length subsets (10-, 30-, 25-, and 50-meters) taken about the centre of the 70-meter segment.

[Table 2 near here].

The relative margin-of-error (MOE) for the distribution of N_T random variables (Papoulis 1991), with significance α within a (1-α)% confidence interval, $MOE_{(1-\alpha)}$, is

$$MOE_{1-\alpha} = \pm \frac{\sigma \times t_{1-\alpha/2,df}}{\mu \sqrt{N_T}} \tag{11}$$

The t-score for a normalized cumulative t-distribution with df degrees of freedom is $t_{1-\alpha/2,df}$. The mean value of the variables is μ, and σ is the standard deviation. Hence,

MOE_{95} is a relative measure of the amount of spread about the mean value for samples that fall within the 95% confidence interval. For example, the row before the last row of Table 2 indicates that for the 50-meter segment, there was a 1.34% MOE_{95} in measuring the RIF-index. Furthermore, a 2.8% variation in speed (standard deviation/mean) accounted for 31.7% of the error, but the residual factors dominated at 68.3% contribution.

Table 3 summarizes the error in GPS position tags relative to the geo-fence. The mean error L_μ from the inertial profiler experiments were a factor (Δ_μ) of 1.36 times greater than the mean error from the prior experiments using the Chevrolet Traverse. Similarly, the six-sigma error spread L_σ was a factor (Δ_σ) of 2.35 times greater.

[Table 3 near here].

The proportional contribution of residual factors η_E^L to the spread in RIF-indices was more substantial for the inertial profiler experiments. The speed coefficient of variation (CV), $\sigma_{\bar{v}} / \bar{\bar{v}}$ for the Chevrolet Traverse was a factor of 2.31 times greater than the speed CV for the inertial profiler. However, the error from residual factors, particularly GPS tagging errors, dominated in both cases. In fact, the use of a smartphone speed sensor may have even resulted in an over-estimation of the relative contribution from speed errors. Therefore, using an actual connected vehicle speed sensor will retain the conclusion that errors from residual factors dominate.

In addition to validating the expectations from the theoretical development, these experiments reveal the degree of relative sensitivities to each of the dominant factors that users should expect in practice.

4 Results and discussion

Figure 2 plots the histogram of RIF-indices calculated from the inertial profiler (table 1) and the 2011 Chevrolet Traverse for the 70-meter traversal path length (table 2). It is evident that the mean values of the distributions practically agree. That is, the mean RIF-index from the inertial profiler and the Chevrolet Traverse were 0.179 and 0.181, respectively. Speed variations from the inertial profiler contributed only 1.7% to the spread in RIF-indices whereas the traversal path variations from GPS position tagging errors contributed 98.3% to the error spread (table 3). GPS tagging errors were less severe for the experiments involving the Chevrolet Traverse, but there was more speed variation. Hence, speed variations contributed substantially more (39%) to the spread in RIF-indices from the Chevrolet Traverse. Nevertheless, in both cases the residual errors η_{E}^{L} dominated. This reciprocal relationship in residual error contributions from the spread in GPS position tagging L_σ relative to speed variations validates the expectation from equation (9).

[Figure 2 near here].

Figure 2 also plots the least squares fits of a Student *t*-distribution to the histograms. The *t*-distribution is appropriate for hypothesis testing of fewer than 30 samples, and approaches the Gaussian distribution for larger sample sizes (Agresti and Finlay 2009). The significance value for a chi-squared test statistic (χ^2) of the agreement with the fit is

$$\chi^2 = \sum_{k=1}^{n} \frac{(O_k - E_k)^2}{E_k}. \tag{12}$$

The random variables O_k are the histogram values observed in bin k and E_k are the expected values of the hypothesized distribution. The significance values for RIF-indices from the inertial profiler and Chevrolet Traversal samples were 77.9% and 98.4%, respectively.

Therefore, the chi-squared tests cannot reject the hypothesis that the distribution of RIF-indices follows the classic distribution because the significance values are much greater than 5%. This result provides confidence that the precision will continue to increase with the ever-increasing traversal volume of connected vehicles.

Figure 3a provides further evidence that the MOE_{95} for both the IRI and the RIF-index diminishes with increasing traversal volume. The MOE_{95} for RIF-indices diminished below 1.5% as the traversal volume approached 50. In fact, for the 70-meter segment, the RIF-transform achieved the same level of precision as the IRI procedure (4.4%) within seven traversals. Reducing the segment length by half increased the influence from GPS tagging errors as expected. Consequently, the RIF-index for the shorter segment required more than double the number of traversals (from 7 to 17) to achieve the same level of precision as the IRI procedure. Figure 3b plots the MOE_{95} for the RIF-indices (left axis) as a function of segment length. The exponential decrease to a point of diminishing returns indicates that the influence from GPS errors wane substantially for segment lengths that are greater than 50-meters. The proportional contribution from residual errors (right axis) diminishes exponentially from nearly 100% for 10-meter long segments to approximately 61% for the 70-meter long segments.

[Figure 3 near here].

Overall, this result indicates that the larger traversal volumes from connected vehicle environments will yield ever-increasing levels of precision for any segment length, but the consistency will improve more rapidly for segments longer than 50 meters.

5 Summary and conclusions

Affordable and scalable methods of measuring localized roughness enable improved efficiencies and effectiveness in the practice of pavement asset management. However, the prevalent approach that relies on laser-based inertial profilers and the IRI is relatively expensive to deploy for continuous network level evaluations. Connected vehicle methods provide an attractive alternative, but the approach requires higher traversal volume to achieve the same level of precision as the IRI procedure. This study characterized the error contributors for the connected vehicle approach and conducted case studies to assess the conditions needed to achieve a desired level of consistency.

The IRI achieves relatively high precision within few traversals because the procedure that produces the index uses a fixed quarter-car and a precise traversal speed. Conversely, connected vehicles rely on geo-fence triggering based on the geospatial position estimates from on-board GPS receivers. Therefore, variations in position tagging the inertial data stream lead to larger variations in the longitudinal traversal path analysed. Additionally, the roughness index derived from connected vehicle data reflects variations in the actual vehicle suspension behaviour, traversal speed, and sensor parameters. The field studies conducted found that the connected vehicle approach could achieve the same level of precision as the IRI procedure within 7 traversals. The results further indicate that for a given vehicle and segment lengths larger than 50-meters, the margin-of-error in estimating RIF-indices diminished below 1.5% as the traversal volume exceed 50.

Future research will utilize the connected vehicle method to examine the wavelength composition of different pavement types and establish a relationship with the power spectral density reported using the IRI procedure.

References

The authors would also like to express their sincere appreciation to Mr. Thomas Burchett of Fugro Roadware for his contribution in data collection at MnROAD facilities.

References

Agresti, A., and Finlay, B., 2009. *Statistical Methods for the Social Sciences*. 4th. City: Upper Saddle River: Pearson Prentice Hall

Ahlin, K. and Granlund, N.J., 2002. Relating road roughness and vehicle speeds to human whole body vibration and exposure limits. *Int. J. Pavement Eng.,* 3 (4), 207-216.

Ayenu-Prah, A.Y. and Attoh-Okine, N.O., 2009. Comparative study of Hilbert–Huang transform, Fourier transform and wavelet transform in pavement profile analysis. *Vehicle Syst. Dyn.,* 47 (4), 437-456.

Bridgelall, R., 2014a. Connected vehicle approach for pavement roughness evaluation. *J. Infrastruct. Syst.,* 20 (1), 1-6.

Bridgelall, R., 2014b. Inertial sensor sample rate selection for ride quality measures. *J. Infrastruct. Syst.,* 21 (2), 1-5.

Bridgelall, R., 2014c. A participatory sensing approach to characterize ride quality. In: J.P. Lynch, K-W. Wang, and H. Sohn, ed. *Proc. SPIE 9061, Sensors and smart structures technologies for civil, mechanical, and aerospace systems*, 8 March 2014, San Diego. Bellingham: International Society for Optics and Photonics (SPIE).

Bridgelall, R,. 2015. Precision bounds of pavement distress localization with connected vehicle sensors. *J. Infrastruct. Syst.,*21 (1) 1-7.

Bridgelall, R., Huang Y., Zhang Z., and Deng F., 2016. Precision enhancement of pavement roughness localization with connected vehicles. *Meas. Sci. Technol*., 27 (2) 025012.

Byrne, M., Parry, T., Isola, R., and Dawson, A., 2013. Identifying road defect information from smartphones. *Road Transp. Res.,* 22 (1), 39-50.

Dawkins, J., Bevly, D., Powell, B., and Bishop, R., 2011. *Investigation of Pavement Maintenance Applications of Intellidrive.* Pooled Fund Study, Charlottesville, Virginia: University of Virginia.

Du, Y., Liu, C., Wu, D., and Jiang, S., 2014. Measurement of International Roughness Index by using z-axis accelerometers and GPS. *Math. Probl. Eng.,* (2014), 1-10.

Islam, S., Buttlar, W.G., Aldunate, R.G., and Vavrik, W.R., 2014. Measurement of pavement roughness using Android-based smartphone application. *Transport Res. Rec.,* (2457), 30-38.

Karamihas, S.M., 2015. *Measuring, Characterizing, and Reporting Pavement Roughness of Low-Speed and Urban Roads.* Research in Progress, Washington, D.C.: Transportation Research Board of the National Academies. Accessed October 12, 2015. http://apps.trb.org/cmsfeed/TRBNetProjectDisplay.asp?ProjectID=3404.

Lak, M.A., Degrande, G., and Lombaert, G., 2011. The influence of the pavement type on ground-borne vibrations due to road traffic. In: G. De Roeck, G. Degrande, G. Lombaert and G. Müller, ed. *Proc. 8th Intl. Conf. on Structural Dynamics.* Leuven, Belgium: EURODYN 2011. 777-784.

MnROAD, 2015. *Safer, Smarter, Sustainable Pavements Through Innovative Research.* Brochure, Monticello, MN: Minnesota Department of Transportation.

Nomura, T., and Shiraishi, Y., 2015. A method for estimating road surface conditions with a smartphone. *Int. J. Informatics Society,* 7 (1), 29-36.

Papagiannakis, A.T., 1997. The Need for a New Pavement Roughness Index; RIDE. *International Truck & Bus Meeting & Exposition.* Washington, D.C.: Society of Automotive Engineers International.

Papoulis, A., 1991. *Probalility, random variables, and stochastic processes.* New York: McGraw-Hill.

Rajamohan, D., Gannu, B., and Rajan, K.S., 2015. MAARGHA: a prototype system for road condition and surface type estimation by fusing multi-sensor data. *ISPRS Int. J. Geo-Information,* 4 (3), 1225-1245.

Zhou, Z., Liu, W.Q., Huang, Y., Wang, H.P., Huang, M.H., and Ou, J.P., 2012. Optical fiber Bragg grating sensor assembly for 3D strain monitoring and its case study in highway pavement. *Mech. Syst. Signal Pr.*, 28 (4), 36-49.

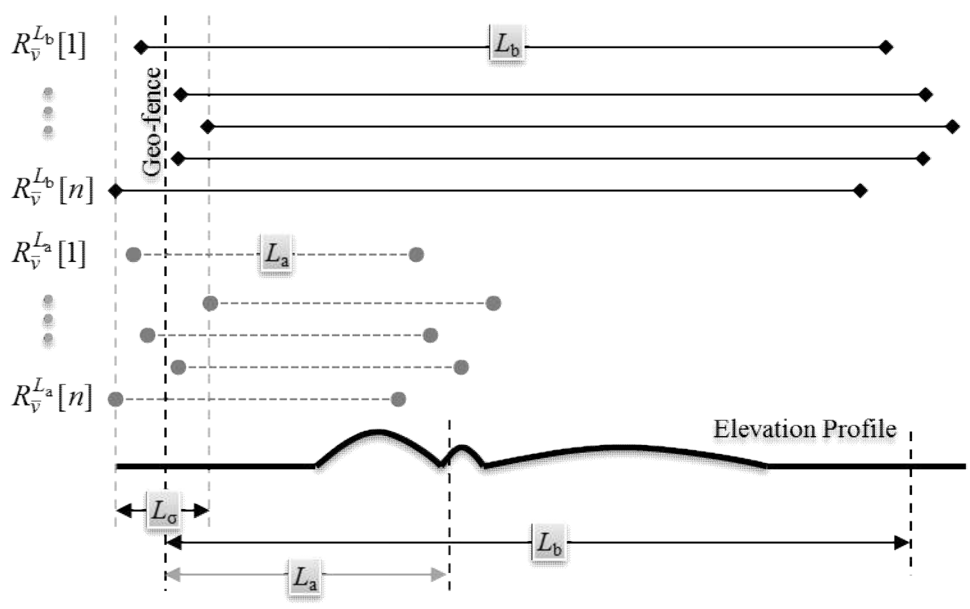

Figure 1. Measurement variability decreases with longer analysis segments.

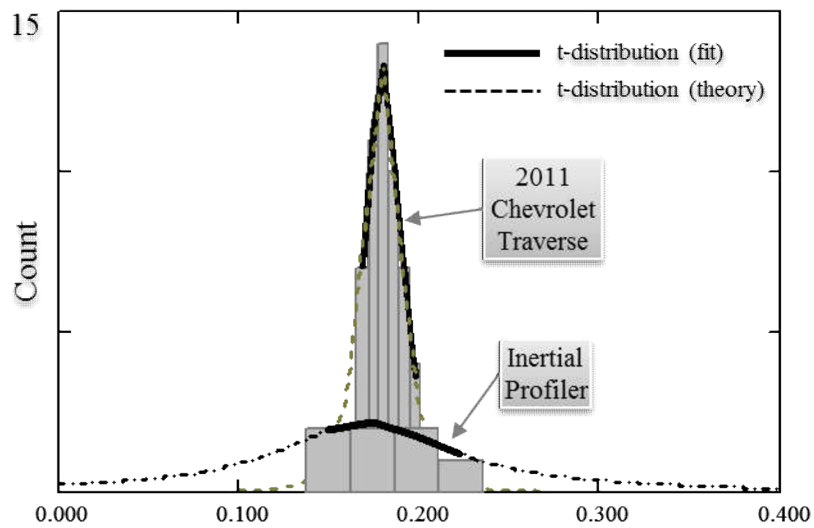

Figure 2. Distribution of RIF-indices from each vehicle for the 70-meter segment.

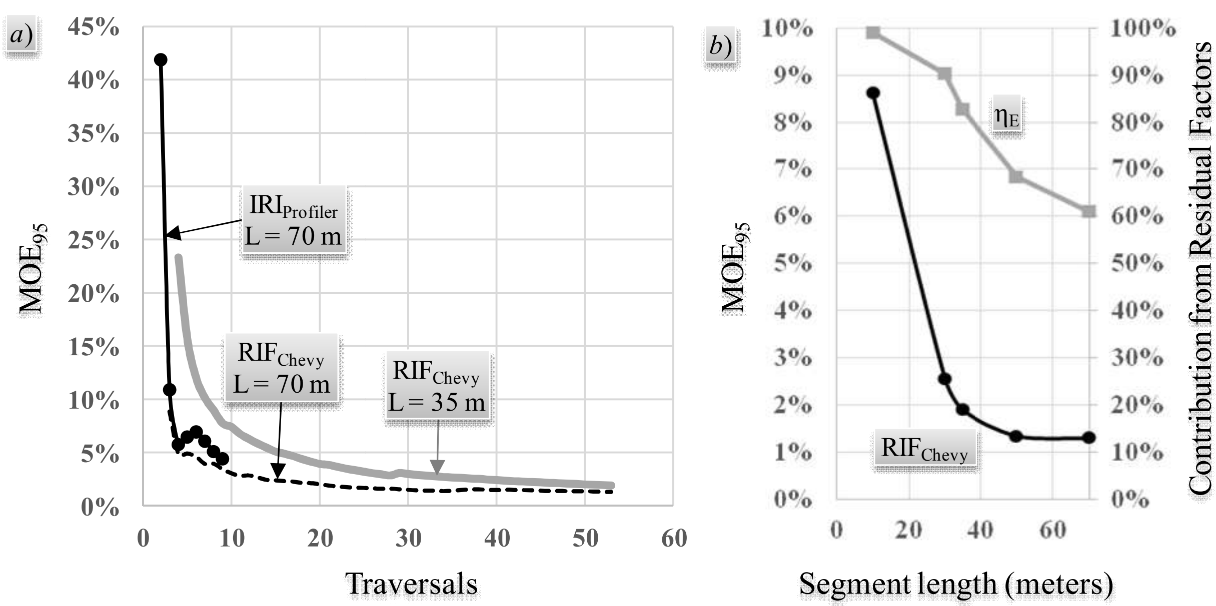

Figure 3. Margin-of-error as a function of traversal volume and segment length.

Table 1. Roughness characterizations from the inertial profiler.

N	IRI (m/km)	R_{80}^{70} (g/m)	$\bar{v}$ (m s^{-1})	σ_v (m s^{-1})
1	1.794	0.176	22.91	0.07
2	1.925			
3	1.795	0.177	22.51	0.22
4	1.828	0.186	22.84	0.30
5	1.664	0.137	22.35	0.04
6	1.640	0.195	22.01	0.38
7	1.648	0.150	22.70	0.44
8	1.725	0.235	21.50	0.44
9	1.739			

Table 2. Roughness characterization from the Chevrolet Traverse.

L (m)	R_{68}^{L} (g/m)	σ_R^L (g/m)	MOE$_{95}$ (%)	$\bar{\bar{v}}$ (m s^{-1})	$\sigma_{\bar{v}}$ (m s^{-1})	$\bar{E}_{gz}^{L}$ (Joules)	η_v^L (%)	η_E^L (%)
10	0.251	0.079	8.63	18.75	0.559	194.6E-6	1.0	99.0
30	0.225	0.021	2.56	18.74	0.541	145.5E-6	9.7	90.3
35	0.218	0.015	1.89	18.74	0.537	135.5E-6	17.4	82.6
50	0.198	0.010	1.34	18.73	0.532	111.9E-6	31.7	68.3
70	0.181	0.008	1.29	18.71	0.518	93.0E-6	39.0	61.0

Table 3. Position error in GPS reference tags from the 70-meter segment traversals.

Probe Vehicle	N	L_μ (m)	L_σ (m)	Δ_μ (m)	Δ_σ (m)	$\bar{\bar{v}}$ (m s^{-1})	$\sigma_{\bar{v}}$ (m s^{-1})	η_v^L (%)	η_E^L (%)
Inertial Profiler	7	8.32	18.81	1.4	2.3	22.40	0.27	1.7	98.3
Chevrolet Traverse	53	6.12	8.01	1.0	1.0	18.71	0.52	39.0	61.0